Model-driven Deep Attention Network for Ultra-fast Compressive Sensing MRI Guided by Cross-contrast MR Image

Yan Yang*, Na Wang*, Heran Yang, Jian Sun(✉), and Zongben Xu

Xi'an Jiaotong University, Xi'an, 710049, China
{yangyan92,nawang2018,yhr.7017}@stu.xjtu.edu.cn,
{jiansun,zbxu}@xjtu.edu.cn

Abstract. Speeding up Magnetic Resonance Imaging (MRI) is an inevitable task in capturing multi-contrast MR images for medical diagnosis. In MRI, some sequences, e.g., in T2 weighted imaging, require long scanning time, while T1 weighted images are captured by short-time sequences. To accelerate MRI, in this paper, we propose a model-driven deep attention network, dubbed as MD-DAN, to reconstruct highly undersampled long-time sequence MR image with the guidance of a certain short-time sequence MR image. MD-DAN is a novel deep architecture inspired by the iterative algorithm optimizing a novel MRI reconstruction model regularized by cross-contrast prior using a guided contrast image. The network is designed to automatically learn cross-contrast prior by learning corresponding proximal operator. The backbone network to model the proximal operator is designed as a dual-path convolutional network with channel and spatial attention modules. Experimental results on a brain MRI dataset substantiate the superiority of our method with significantly improved accuracy. For example, MD-DAN achieves PSNR up to 35.04 dB at the ultra-fast 1/32 sampling rate.

Keywords: Multi-contrast MRI · Prior learning · Model-driven net.

1 Introduction

Magnetic Resonance Imaging (MRI) is a leading biomedical imaging technology, which depicts both anatomical and functional information for disease diagnosis. A typical MRI protocol comprises multi-contrast sequences of same anatomy which provide complementary information to enhance clinical diagnosis. For instance, T1 Weighted Imaging (T1WI) is useful for delineation of morphological information including assessing the gray and white matter and identifying fatty tissue. T2 Weighted Imaging (T2WI) is useful for delineation of edema and inflammation. Fluid Attenuated Inversion Recovery (FLAIR) is useful for suppressing cerebrospinal fluid (CSF) effects on the image to detect the periventricular hyperintense lesions in brain imaging. However, a major challenge in

* Both authors contributed equally to this work.

MRI is its long data acquisition time, for example, typical scanning time for T1WI, T2WI and FLAIR is about 20 mins, limiting its clinical applications in fetal imaging or dynamic imaging. In clinical routines, some contrast sequences such as T1WI, requiring short repetition time (TR) and echo time (TE), allow full sampling, while others, such as T2WI and FLAIR, requiring long TR and TE, can be accelerated by under-sampling. In this paper, we aim to reconstruct highly under-sampled long-time sequence MR image (e.g., T2WI) with the guidance of a certain short-time sequence MR image (e.g., T1WI) [26].

Compressive sensing MRI (CS-MRI) [16] is a predominant approach to accelerate MRI by under-sampling in k-space. Traditional model-based CS-MRI methods rely on regularization related to image prior to improve reconstruction quality, e.g., Total Variation (TV) [3, 10], wavelet regularization [10, 15], nonlocal regularization [7, 20] and dictionary learning [21, 28]. However, it is challenging to handcraft an optimal regularizer. Recently, deep learning method has been applied to CS-MRI. Wang et al. [24] first trained a deep CNN to learn the mapping to high-quality reconstructed images. [13] proposed a multi-scale residual learning network (i.e., U-net) for image reconstruction by removing aliasing artifacts. [6, 9, 17, 23, 27] introduced imaging model or data consistency term to deep networks to learn the priors of images from training data and greatly improve reconstruction accuracy. All these CS-MRI methods consider reconstruction of MRI images with a single contrast (e.g., T1WI, T2WI or FLAIR).

An alternative way to accelerate MRI is to synthesize missing contrast MR image from other contrast with fully-sampled acquisitions. They either learn a dictionary or sparse representation of source contrast patches for target contrast [11, 22], or directly learn a mapping from source to target contrast by a deep neural network [4, 5, 12, 14]. However, such methods suffer from low-quantity reconstruction without requiring samples in k-space. Recently, Xiang et al. [26] proposed a Dense-Unet to accelerate MRI by reconstruction using both under-sampled k-space data and guided MR image. They use a deep network to fuse under-sampled T2WI image and guided fully-sampled T1WI image, and output the reconstructed high quality T2WI MR image.

To reconstruct MR image from its under-sampled k-space acquisitions with guided cross-contrast MR image, we propose a novel interpretable deep attention network by integrating the k-space data constraint and cross-modality relations into a single deep architecture. Specifically, we first propose a novel MR image reconstruction model consisting of a data fidelity term based on k-space data and a cross-contrast prior term modeling relations between contrasts. Then we design an iterative algorithm based on half-quadratic splitting to minimize the model by alternately performing guided image fusion and image reconstruction. To learn the cross-contrast prior from training data, we substitute its proximal operator in the iterative algorithm by a novel backbone network, namely DPA-FusionNet, which is a dual-path convolutional network with channel and spatial attention. Finally, we unfold the iterative algorithm to be a deep architecture, dubbed as *model-driven deep attentation network (MD-DAN)*, as shown in Fig. 1. Experiments on a brain MRI dataset show that our proposed MD-DAN can

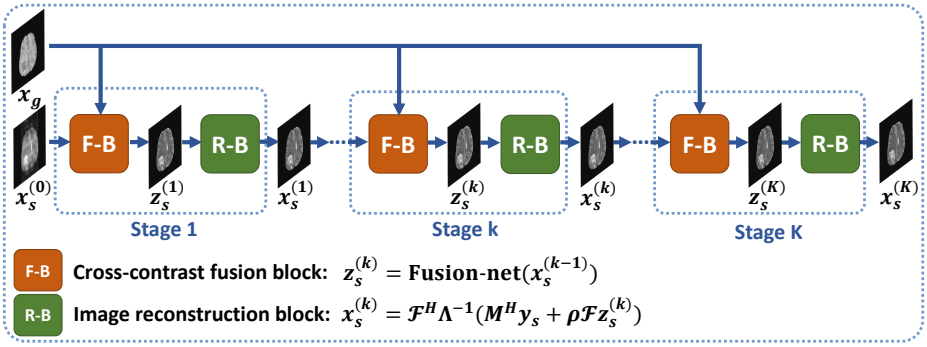

Fig. 1: Illustration of model-driven deep attention network, i.e., MD-DAN. Each stage consists of a cross-contrast fusion block (i.e., F-B) and an image reconstruction block (i.e., R-B). Given a reconstructed image by zero-filling (i.e., $x_s^{(0)}$) and a guided image (i.e., x_g), it outputs reconstructed MR image after K stages.

effectively reconstruct MR image with state-of-the-art reconstruction accuracy even in ultra-fast 1/32 sampling rate.

2 Method

Given under-sampled k-space data $\{y_s \in \mathbb{C}^U\}$ of long-time sequence MR image (e.g., T2WI), and fully sampled reconstructed MR image $\{x_g \in \mathbb{C}^N\}$ of short-time sequence (e.g., T1WI) as guidance, we aim to reconstruct the MR image $\{x_s \in \mathbb{C}^N\}$ from k-space data $\{y_s \in \mathbb{C}^U\}$, where N and U denote the cardinality of MR image and sampled k-space data. Based on the MR imaging mechanism, we design the following MRI reconstruction model:

$$x_s^* = \arg\min_{x_s} \frac{1}{2}||M\mathcal{F}x_s - y_s||_2^2 + \lambda f(x_s, x_g), \tag{1}$$

where $\mathcal{F} \in \mathbb{C}^{N\times N}$ is the Fourier transform and $M \in \mathbb{C}^{U\times N}$ $(U < N)$ is the sampling matrix in k-space. The first term is a data term that enforces data consistency between reconstructed MR image x_s and its under-sampled data y_s in k-space. The second term is a *cross-contrast prior* that models the correlation between MR image x_s and guided image x_g. For example, $f(x_s, x_g)$ can be taken as joint TV, group wavelet-sparsity [10], weighted similarity of intensity [25] or similarity of image patches between multi-contrast MR images [20].

In this work, we aim to learn this prior instead of handcrafting it. To this end, we first design an iterative optimization algorithm for solving Eqn. (1), where the prior will be transformed to be a proximal operator in the iterative algorithm. We then design a novel fusion network with two contrasts as inputs to replace this proximal operator to implicitly learn the cross-contrast prior. The iterative algorithm can be taken as a deep network and trained end-to-end.

2.1 Model Optimization

The reconstruction model of Eqn. (1) can be solved efficiently by half-quadratic splitting (HQS) algorithm [8]. By introducing an auxiliary MR image z_s, s.t., $z_s = x_s$, Eqn. (1) is equivalent to optimizing the following energy model:

$$\arg\min_{z_s, x_s} \frac{1}{2}||M\mathcal{F}x_s - y_s||_2^2 + \lambda f(z_s, x_g) + \frac{\rho}{2}||x_s - z_s||_2^2, \tag{2}$$

where penalty coefficient $\rho \to \infty$ during optimization. The energy model of Eqn. (2) can be minimized by iteratively estimating the unknown variables z_s and x_s. At k-th iteration, we solve the following two subproblems.

Estimating z_s by proximal operator: Given MR image $x_s^{(k-1)}$ at iteration $k-1$, auxiliary MR image z_s can be updated with guided MR image x_g by:

$$z_s^{(k)} = \arg\min_{z_s} \frac{\rho}{2}||x_s^{(k-1)} - z_s||_2^2 + \lambda f(z_s, x_g). \tag{3}$$

By definition of proximal operator of a regularizer term $g(\cdot)$, i.e., $\text{Prox}_{\eta g}(v) = \arg\min_u \frac{1}{2}||v-u||_2^2 + \eta g(u)$, auxiliary image z_s is updated by optimizing Eq. (3):

$$z_s^{(k)} = \text{Prox}_{\frac{\lambda}{\rho} f(\cdot, x_g)}(x_s^{(k-1)}), \tag{4}$$

where proximal operator $\text{Prox}_{\frac{\lambda}{\rho} f(\cdot, x_g)}$ is a nonlinear mapping determined by cross-contrast prior $f(z_s, x_g)$, and maps input MR image $x_s^{(k-1)}$ to $z_s^{(k)}$ with guidance of guided MR image x_g. x_s is initialized by zero-filling: $x_s^{(0)} = \mathcal{F}^H M^H y_s$.

Estimating x_s by image reconstruction: Given updated auxiliary MR image $z_s^{(k)}$ at iteration k, reconstructed MR image x_s can be updated as:

$$x_s^{(k)} = \arg\min_{x_s} \frac{1}{2}||M\mathcal{F}x_s - y_s||_2^2 + \frac{\rho}{2}||x_s - z_s^{(k)}||_2^2. \tag{5}$$

This sub-problem has a closed-form solution:

$$x_s^{(k)} = \mathcal{F}^H \Lambda^{-1}(M^H y_s + \rho \mathcal{F} z_s^{(k)}), \tag{6}$$

where $\Lambda = M^H M + \text{diag}(\rho)$ is a diagonal matrix.

By iteratively updating auxiliary and reconstructed MR images using Eqns. (4) and (6), cross-contrast prior is imposed on x_s by proximal operator in Eqn. (4) with guidance of MR image x_g.

2.2 Unfolded Network for Cross-contrast Prior Learning

We unfold the iterative algorithm (Eqns. (4), (6)) to be a deep architecture, dubbed *MD-DAN*. As illustrated in Fig. 1, the whole network contains K stages, each of which corresponds to one iteration with two blocks, i.e., **cross-contrast fusion block (F-B)** and **image reconstruction block (R-B)**, implementing updates of variable z_s and x_s in Eqn. (4) and Eqn. (6) respectively.

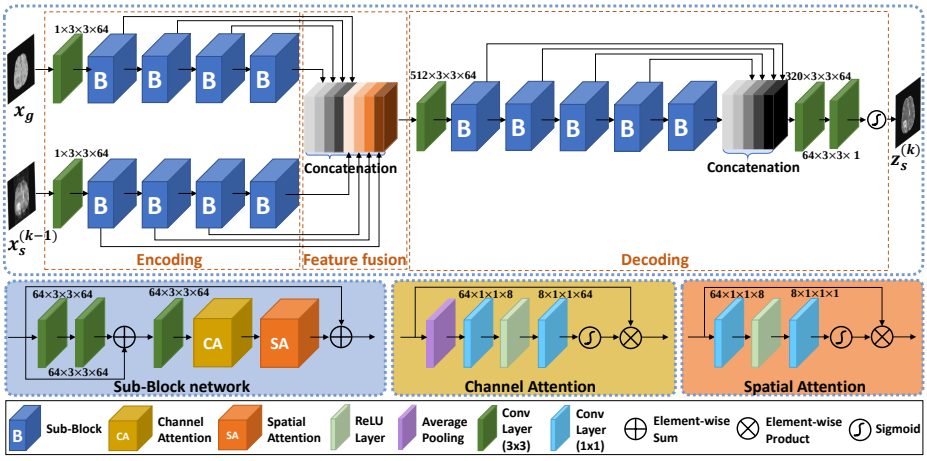

Fig. 2: The network structure of cross-contrast fusion network (DPA-FusionNet).

Cross-contrast fusion block. Instead of handcrafting cross-contrast prior $f(\cdot,\cdot)$, we substitute its proximal operator in Eqn. (4) by a learnable network:

$$z_s^{(k)} = \text{Prox}_{\frac{\lambda}{\rho} f(\cdot, x_g)}(x_s^{(k-1)}) \triangleq \textbf{Fusion-net}(x_s^{(k-1)}, x_g). \tag{7}$$

The Fusion-net is to fuse two contrast images as inputs and output updated auxiliary MR image. As shown in Fig. 2, it is designed as a dual-path net including encoding, feature fusion and decoding blocks. Encoding block extracts features from guided image x_g and reconstructed image in $(k-1)$-th stage (i.e., $x_s^{(k-1)}$) by two sub-encoders, each of which consists of a convolution and four cascaded Sub-Block networks. Then features of different layers of encoding networks from different contrasts are concatenated and further fused by a decoding network consisting of a convolution, five cascaded Sub-Blocks, a multi-scale feature fusion (i.e., feature concatenation) followed by two convolution and a sigmoid operation, and the decoder outputs the updated auxiliary MR image $z_s^{(k)}$. We name this cross-contrast fusion network as *Dual Path Attention Fusion Network* (*DPA-FusionNet*). Please see Fig. 2 for detailed network hyper-parameters.

Each Sub-Block network, as shown in Fig. 2, is designed with skip connection, channel attention (CA) [29] and spatial attention (SA) [19] modules. The two attention modules are introduced as follows.

Channel attention (CA). Channel attention module is to make network pay more attention to important channel features from different contrasts. Firstly, we convert features denoted by F into a channel descriptor denoted by G through average pooling channel-by-channel: $G_c = \frac{1}{H \times W} \sum_i \sum_j F_c(i,j)$, where F_c is feature in c-th channel, and H and W are the height and width of the features. Then the channel descriptor G goes through the cascaded layers: Conv $\rightarrow$ ReLu $\rightarrow$ Conv $\rightarrow$Sigmoid, and we get weights of different channels W^{CA}. Finally, weights are applied to the input features by element-wise product: $F_c^{out} = W_c^{CA} \otimes F_c$.

Spatial attention (SA). Spatial attention module is to force network to pay more attention to important spatial regions of image, such as high-frequency and heavy artifact areas. For the features F, we get weights of different pixels W^{SA} by cascaded layers: Conv $\rightarrow$ ReLu $\rightarrow$ Conv $\rightarrow$Sigmoid. Then weights are applied to the input features by element-wise product: $F_c^{out} = W^{SA} \otimes F_c$.

2.3 Network Training

We use mean squared error (MSE) loss to train the net: $\mathcal{L}(\Theta) = \sum_n ||x_n^{(K)}(\Theta) - x_n^{gt}||_2$, where $x_n^{(K)}(\Theta)$ is the network output for n-th data, Θ are network parameters of MD-DAN with backbone DPA-FusionNets in different stages initialized by Xavier random initialization. x_n^{gt} is targeting MR image reconstructed from fully-sampled k-space data. ρ is initialized as 1e-5. The backbone network at different stages does not share parameters. We implement and train MD-DAN by PyTorch using Adam with learning rate of 1e-4, on an Ubuntu 16.04 system with GTX 1080 Ti GPU. We conduct stage-wise training followed by an end-to-end fine tuning, and we train the network in each stage for 120 epochs.

3 Experiments

Experimental settings. We evaluate MD-DAN on brain MR images from BraTS 2019 dataset[1] [1, 2, 18], providing clinically-acquired multi-contrast MRI scans of glioblastoma patients from 19 institutions. We respectively take 190 and 189 subjects as training and test set. We train our MD-DAN to reconstruct T2WI MR image from its under-sampled k-space data with guidance of T1WI image. Successive 2D slices are used to train MD-DAN and test accuracy is performed on whole 3D volume in size of $240 \times 240 \times 115$. Preprocessing steps including N4 corrected and peak normalization were applied. We used 1D Cartesian sampling with sampling rates of 1/8, 1/16 and 1/32 to under-sample T2WI k-space data.

Compared methods. We compare MD-DAN ($K = 4$) with five single contrast CS-MRI methods that reconstruct T2WI MR image from under-sampled k-space data including Zero-filling (ZF), DC-CNN [23], Dense-Unet-R, ResNet-R and DPA-FusionNet-R. We also compare with image synthesis methods including Dense-Unet-S, ResNet-S and DPA-FusionNet-S which synthesize T2WI MR image from T1WI MR image. Dense-Unet-R(S), ResNet-R(S) are respectively based on Dense-Unet (2 down and up sampling operations and 5 dense blocks [26]) and ResNet (9 convolution residual blocks [30]). DPA-FusionNet-R(S) is variant of our DPA-FusionNet in Fig. 2 without upper (for '-R') or lower (for '-S') path respectively for single modality reconstruction and cross-contrast synthesis. We further compare with three reconstruction methods guided by cross-contrast image including model-based method FCSA-MT [10] and two state-of-the-art deep learning networks of Dense-Unet [26] and ResNet [30]. The two deep networks take reconstructed under-sampled T2WI image and fully sampled T1WI image as input, and output the reconstructed T2WI image.

[1] https://ipp.cbica.upenn.edu/

Table 1: Comparison of average performance on the testing dataset.

		1/8 rate		1/16 rate		1/32 rate		
Type	Method	PSNR	nRMSE	PSNR	nRMSE	PSNR	nRMSE	Time
T2→T2	ZF	26.0883	0.3312	25.9763	0.3357	25.0999	0.3719	0.010s
	DC-CNN	35.8136	0.1095	32.2087	0.1665	28.0524	0.2667	0.031s
	Dense-Unet-R	32.1378	0.1698	30.6749	0.1983	28.0846	0.2661	0.014s
	ResNet-R	33.5167	0.1425	31.2695	0.1851	28.4251	0.2565	0.016s
	DPA-FusionNet-R	33.5520	0.1420	31.3854	0.1825	28.5896	0.2516	0.026s
T1→T2	Dense-Unet-S	29.6061	0.2235	29.6061	0.2235	29.6061	0.2235	0.014s
	ResNet-S	30.2969	0.2079	30.2969	0.2079	30.2969	0.2079	0.015s
	DPA-FusionNet-S	30.3193	0.2077	30.3193	0.2077	30.3193	0.2077	0.027s
T1+T2 →T2	FCSA-MT	35.8089	0.1118	32.5788	0.1626	27.6125	0.2844	4.001s
	Dense-Unet	35.4403	0.1147	34.2353	0.1314	32.9811	0.1520	0.015s
	ResNet	36.1856	0.1047	35.0296	0.1264	33.8310	0.1378	0.016s
	MD-DAN	**40.6069**	**0.0639**	**37.9372**	**0.0868**	**35.0364**	**0.1206**	0.108s

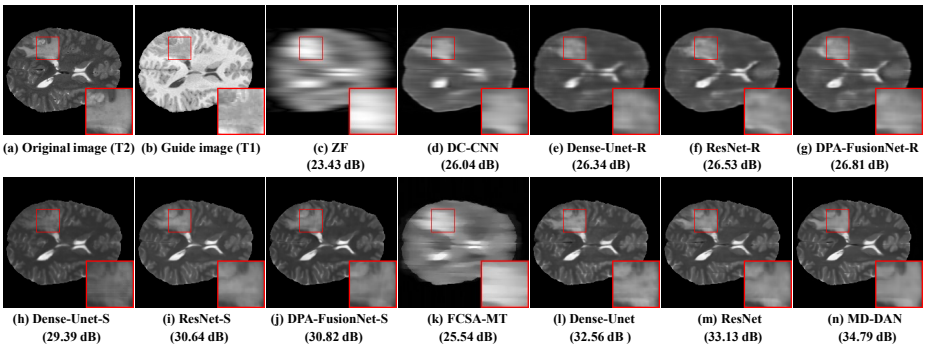

Fig. 3: Results for a brain MR image using 1/32 1D Cartesian sampling.

Results. Table 1 shows the quantitative results on test dataset with 1/8, 1/16 and 1/32 sampling rates. Our MD-DAN significantly outperforms all synthesis-based methods and single contrast reconstruction methods, especially at higher sampling rates 1/16 and 1/32, which verify the effectiveness of joint reconstruction using k-space data and guided image. For example, in 1/16 sampling rate, MD-DAN outperforms DPA-FusionNet-S by 7.62 dB and DC-CNN by 5.73 dB. Compared with Dense-Unet and ResNet in the same setting as ours, our MD-DAN achieves better reconstruction accuracy in PSNR and nRMSE using 50% less sampled data. Examples of reconstructed images by different methods in 1/32 sampling rate are shown in Fig. 3. More examples are in supplementary material. Our method yields higher-quality MR images without obvious artifacts.

Comparisons of different backbone networks. We use a dual-path DPA-FusionNet in Fig. 2 as backbone to replace proximal operator in our model-driven

Table 2: Comparison of average performance with sampling rate of 1/8.

	MD-Dense-Unet	MD-ResNet	MD-DAN
PSNR	39.6798	40.2295	**40.6069**
nRMSE	0.0708	0.0666	**0.0639**
Training time	5.5 days	6 days	7 days

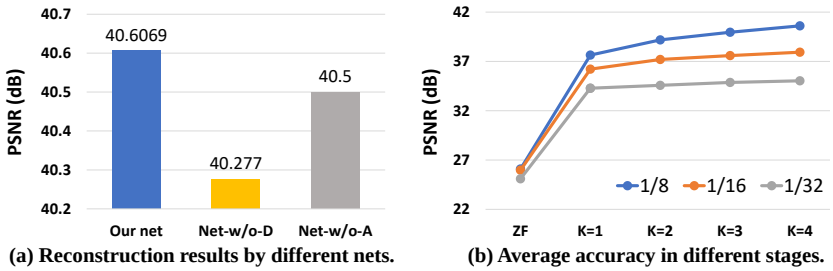

(a) Reconstruction results by different nets. **(b) Average accuracy in different stages.**

Fig. 4: Performance comparison of different network settings

network. To verify superiority of DPA-FusionNet, we also respectively use Dense-Unet and ResNet to replace the proximal operator in our framework, denoted as MD-Dense-Unet and MD-ResNet. Table 2 shows performance with sampling rate of 1/8 in 4 stages. Our MD-DAN with DPA-FusionNet as proximal operator works best and improves the PSNR at least 0.37 dB than others.

Effectiveness of backbone network design. To explore effectiveness of dual-path structure and attention modules in backbone network DPA-FusionNet, we respectively discard either of them in MD-DAN, and the corresponding networks are denoted as Net-w/o-D and Net-w/o-A. The average PSNR values of trained Net-w/o-D and Net-w/o-A with K=4 and 1/8 sampling rate are shown in Fig. 4(a). Dual-path structure and attention modules are both beneficial for improving performance, e.g., the result of MD-DAN is higher in 0.33 dB and 0.11 dB than Net-w/o-D and Net-w/o-A respectively.

Effect of number of stages. To explore influence of the number of stages (i.e., K) on reconstruction accuracy, we train MD-DAN from stage 1 to stage 4 in a greedy way, and the average accuracies on test dataset at different sampling rates and stages are shown in Fig. 4(b). With the increase of stages, the accuracy of reconstruction is improved gradually at all three sampling rates.

4 Conclusion

We proposed a novel model-driven deep attention network to reconstruct highly under-sampled long-time sequence MR image with guidance of a short-time sequence MR image. We design a new reconstruction model with cross-contrast

prior, inspiring us to design a novel deep architecture, in which cross-contrast prior is learned by replacing its proximal operator with a deep DPA-FusionNet. Our method can be extended to other contrast MR image (e.g., FLAIR). We also plan to extend it to simultaneously reconstruct multiple contrast MRI images.

Acknowledgement

This work was supported in part by NSFC under Grants 11971373, 61976173, 11690011, 61721002, U1811461, and in part by the National Key Research and Development Program of China under Grant 2018AAA0102201.

References

1. Bakas, S., Akbari, H., Sotiras, A., Bilello, M., Rozycki, M., Kirby, J.S., Freymann, J.B., Farahani, K., Davatzikos, C.: Advancing the cancer genome atlas glioma mri collections with expert segmentation labels and radiomic features. Nature Scientific data **4**, 170–117 (2017)
2. Bakas, S., Reyes, M., Jakab, A., Bauer, S., Rempfler, M., Crimi, A., Shinohara, R.T., Berger, C., Ha, S.M., Rozycki, M., et al.: Identifying the best machine learning algorithms for brain tumor segmentation, progression assessment, and overall survival prediction in the brats challenge. arXiv (2018)
3. Block, K.T., Uecker, M., Frahm, J.: Undersampled radial mri with multiple coils. iterative image reconstruction using a total variation constraint. Magn. Reson. Med. **57**(6), 1086–1098 (2007)
4. Chartsias, A., Joyce, T., Giuffrida, M.V., Tsaftaris, S.A.: Multimodal mr synthesis via modality-invariant latent representation. IEEE Trans. Med. Imaging **37**(3), 803–814 (2017)
5. Dar, S.U., Yurt, M., Karacan, L., Erdem, A., Erdem, E., Çukur, T.: Image synthesis in multi-contrast mri with conditional generative adversarial networks. IEEE Trans. Med. Imaging **38**(10), 2375–2388 (2019)
6. Duan, J., Schlemper, J., Qin, C., Ouyang, C., Bai, W., Biffi, C., Bello, G., Statton, B., O'Regan, D.P., Rueckert, D.: Vs-net: Variable splitting network for accelerated parallel mri reconstruction. In: MICCAI. pp. 713–722 (2019)
7. Eksioglu, E.M.: Decoupled algorithm for mri reconstruction using nonlocal block matching model: Bm3d-mri. J. Math. Imaging and Vision **56**(3), 430–440 (2016)
8. Geman, D., Yang, C.: Nonlinear image recovery with half-quadratic regularization. IEEE Trans. Image Process. **4**(7), 932–946 (1995)
9. Hammernik, K., et al.: Learning a Variational Network for Reconstruction of Accelerated MRI Data. Magn. Reson. Med. **79**(6), 3055–3071 (2018)
10. Huang, J., Chen, C., Axel, L.: Fast multi-contrast mri reconstruction. Magn. Reson. imaging **32**(10), 1344–1352 (2014)
11. Huang, Y., Shao, L., Frangi, A.F.: Cross-modality image synthesis via weakly coupled and geometry co-regularized joint dictionary learning. IEEE Trans. Med. Imaging **37**(3), 815–827 (2017)
12. Joyce, T., Chartsias, A., Tsaftaris, S.A.: Robust multi-modal mr image synthesis. In: MICCAI. pp. 347–355 (2017)
13. Lee, D., Yoo, J., Ye, J.C.: Deep residual learning for compressed sensing mri. In: IEEE ISBI. pp. 15–18 (2017)

14. Li, H., Paetzold, J.C., Sekuboyina, A., Kofler, F., Zhang, J., Kirschke, J.S., Wiestler, B., Menze, B.: Diamondgan: Unified multi-modal generative adversarial networks for mri sequences synthesis. In: MICCAI. pp. 795–803 (2019)
15. Lustig, M., Donoho, D., Pauly, J.M.: Sparse mri: The application of compressed sensing for rapid mr imaging. Magn. Reson. Med. **58**(6), 1182–1195 (2007)
16. Lustig, M., Donoho, D.L., Santos, J.M., Pauly, J.M.: Compressed sensing mri. IEEE Signal Process. Mag. **25**(2), 72–82 (2008)
17. Meng, N., Yang, Y., Xu, Z., Sun, J.: A prior learning network for joint image and sensitivity estimation in parallel mr imaging. In: MICCAI. pp. 732–740 (2019)
18. Menze, B.H., Jakab, A., Bauer, S., Kalpathy-Cramer, J., Farahani, K., Kirby, J., Burren, Y., Porz, N., Slotboom, J., Wiest, R., et al.: The multimodal brain tumor image segmentation benchmark (brats). IEEE Trans. Med. Imaging **34**(10), 1993–2024 (2014)
19. Qin, X., Wang, Z., Bai, Y., Xie, X., Jia, H.: Ffa-net: Feature fusion attention network for single image dehazing. In: AAAI (2020)
20. Qu, X., Hou, Y., Lam, F., Guo, D., Zhong, J., Chen, Z.: Magnetic resonance image reconstruction from undersampled measurements using a patch-based nonlocal operator. Med. Image Anal. **18**(6), 843–856 (2014)
21. Ravishankar, S., Bresler, Y.: Mr image reconstruction from highly undersampled k-space data by dictionary learning. IEEE Trans. Med. Imaging **30**(5), 1028–1041 (2010)
22. Roy, S., Carass, A., Prince, J.L.: Magnetic resonance image example-based contrast synthesis. IEEE Trans. Med. Imaging **32**(12), 2348–2363 (2013)
23. Schlemper, J., et al.: A Deep Cascade of Convolutional Neural Networks for Dynamic MR Image Reconstruction. IEEE Trans. Med. Imaging **37**(2), 491–503 (2018)
24. Wang, S., Su, Z., Ying, L., Xi, P., Dong, L.: Accelerating magnetic resonance imaging via deep learning. In: IEEE ISBI. pp. 514–517 (2016)
25. Weizman, L., Eldar, Y.C., Ben, B.D.: Reference-based mri. Medical physics **43**(10), 5357 (2016)
26. Xiang, L., Chen, Y., Chang, W., Zhan, Y., Lin, W., Wang, Q., Shen, D.: Ultra-fast t2-weighted mr reconstruction using complementary t1-weighted information. In: MICCAI. pp. 215–223 (2018)
27. Yang, Y., Sun, J., Li, H., Xu, Z.: Deep admm-net for compressive sensing mri. In: NIPS, pp. 10–18 (2016)
28. Zhan, Z., Cai, J.F., Guo, D., Liu, Y., Chen, Z., Qu, X.: Fast multiclass dictionaries learning with geometrical directions in mri reconstruction. IEEE Trans. Biomed. Eng. **63**(9), 1850–1861 (2015)
29. Zhang, Y., Li, K., Li, K., Wang, L., Zhong, B., Fu, Y.: Image super-resolution using very deep residual channel attention networks. In: ECCV (2018)
30. Zhu, J.Y., Park, T., Isola, P., Efros, A.A.: Unpaired image-to-image translation using cycle-consistent adversarial networks. In: ICCV. pp. 2223–2232 (2017)